SUPPLEMENTARY MATERIAL

Mapping Methodology

We used the Environmental Systems Research Institute, Inc. (v. 9.3, ®1982-2011, Redlands, CA) ArcGIS software package of as a means to co-register and analyze mapping datasets used in this study. Vector data (i.e., geologic contacts) was digitized as lines using the digital streaming capability available in ArcGIS and subsequently converted to enclosed polygons. Mapping was conducted at a regional scale in support of an ongoing 1:20,000,000 scale global geologic mapping project for Mars (e.g., Tanaka et al., 2012). Current mapping guidelines suggest photogeologic mapping on multiple, scale-specific digital bases should occur at 25% of the publication scale (Tanaka et al., 2009). As such, we mapped at a consistent scale of 1:5,000,000, which allowed for substantially detailed lines for use in both hard-copy manuscript publication as well as a digital supplement while remaining true to the publication map scale of the supporting geologic map. Vertex spacing was controlled in ArcGIS and was set to place spatial points within linework every 5 km meters (1 vertex per 1 millimeter at 1:5,000,000 digitizing map scale).

The primary base for the photogeologic map presented in this study was the Mars Orbiter Laser Altimeter (MOLA) gridded topographic model (463 m/px), MOLA-derived shaded-relief, slope, and aspect maps, and THEMIS IR image mosaics (100 m/px). We mapped the unit based on the (1) identification of topographically subtle convex-upward scarps that enclose discrete, relatively high-standing areas, (2) distribution of these enclosed areas in relation to fields of knobs, mesas, arcuate ridges, and pedestal craters, and (3) apparent superposition of these discrete materials on Late Hesperian and Early Amazonian geologic units. Though the map base provided the contextual information necessary to identify and correlate geologic contacts, we verified these efforts by integrating other data sets, including the full range of THEMIS, CTX, and HiRISE images via web-linked image footprints in the project GIS. Though these data sets provided important information regarding unit texture and stratigraphic relationships, they were considered supplemental because they did not provide complete areal coverage at map scale.

The MOLA gridded data set was used to assess unit thickness due to its ease of use over large regions (compared to the data intensive and unwieldy nature of the MOLA PEDR standard data product). A question arises, then, regarding the vertical reliability of the interpolated (gridded) data when determining subtle heights of unit mAl above surrounding terrains, as presented herein. Neumann et al. (2001) noted that the vertical and horizontal accuracy of both MOLA standard and gridded data products are tightened by adjusting differences between altimetry measurements acquired at a common location on distinct orbital tracks (i.e., cross-over analysis and corrections). Therein, MOLA gridded products helped to highlight occasional meter-level mis-registrations between adjacent tracks and points requiring >40 m vertical adjustment were deemed unreliable and rejected for interpolation (Neumann et al, 2001). Adjusted shot track altimetry resulted in a topographic model whose vertical accuracy is typically better than 1 m (Neumann et al., 2001). Cross-over corrections and the number of points per cell in the gridded product indicate that the use of MOLA PEDR standard data products is unlikely to alter the thickness results reported herein.

Crater Counting Methodology

We selected 24 sites for crater counting, shown in Supplement Figure 1. However, of these, only 4 sites were suited to produced statistically meaningful model ages. The remaining sites were unsuited for crater analysis due to one or more of the following reasons: (1) the presence of obscuring secondary crater fields, (2) the presence of thumbprint terrain, where impact craters are difficult to differentiate from small conical structures, (3) the presence of sublimation pits wherein buried or excavated impact features are morphologically inseparable and/or wherein measured crater diameters are not tightly constrained, (4) the lack of a suitable number of impact craters required to derive model ages, and (5) the presence of large proportions of buried or excavated impact features, wherein the original crater diameter is not tightly constrained. Examples of these limitations are provided in supplemental material as representative crater plots.

Crater-Based Thickness Estimates

Estimates of the thickness of particular geologic units can be made by examining the size-frequency distributions of impact craters on unit surfaces, as applied and reported by Hiesinger et al. (2002) for lunar lava flows and for Platz et al. (2010) for Martian lava flows. If craters of the underlying older unit are visible, a characteristic deflection in the crater size-frequency distribution (CSFD) develops (Platz et al. 2010). This deflection can be used to determine minimum and maximum crater diameters that have been affected by deposition of a younger unit. The diameter ranges over which this deflection occur for the CSFD used in this investigation are reported in supplemental material as Table 1S.

Platz et al. (2010) noted that there are two major sources of error that affect estimates of material thickness using CSFDs: (1) the interdependency of available formulas that describe cavity shape for a range of crater diameters, and (2) the degree of crater degradation over time. The known relationship between Martian crater diameter (*D*) and rim height (*h*) above adjacent terrain used in this study is (Garvin et al., 2002):

$$h = 0.07D^{0.52} \ (D<7\text{km}),$$

which allows us to derive a value for material thickness (Platz et al., 2010). This relationship is based on morphologically "fresh" impact craters (Garvin et al., 2002). As such, material thickness estimates using this value can be overestimated by up to a factor of 2, particularly if a significant hiatus exits between the emplacement of a geologic unit and its underlying topographic surface (Hörz, 1978; Platz et al., 2010). Barlow (1995) determined that erosional degradation of Martian craters result in rim heights that are 25-54% lower than those expected from "fresh" craters, based on measurement of craters located in Maja Valles and Arabia Terra. Similarly, Platz et al. (2010) determined that degradation results in 23-56% lower values than expected. Rim height measurements made using the database of Robbins and Hynek (2012) for craters with D<5 km and located in Martian mid to high northern latitudes (30 – 80° N) are 49% lower than expected. The values are variable but overlapping. As such, we apply a 50% degradation factor to unit thickness estimates made using the crater diameter and rim height relationship of Garvin et al. (2002). The isochron fit range and resulting estimates of unit mAl are presented in supplemental material as Table 1S.

Supplemental References

Barlow, N.G., 1995, The degradation of impact craters in Maja Valles and Arabia, Mars: Journal of Geophysical Research, v. 100, p. 23,307-23,316.

Garvin, J.B., Sakimoto, S.E.H., Frawley, J.J., and Schnetzler, C., 2002, Global geometric properties of martian impact craters: 33 Annual Lunar and Planetary Science Conference, Houston, Texas, abstract 1255.

Hiesinger, H., Head, J.W., III, Wolf, U., Jauman, R., and Neukum, G., 2002, Lunar mare basalt flow units: thicknesses determined from crater size-frequency distributions: Geophysical Research Letters, v. 29, doi: 10.1029/2002GL014847.

Hörz, F., 1978, How thick are lunar mare basalts?: Proceedings of the 9th Lunar and Planetary Science Conference, p. 3311-3331.

Neumann, G.A., Rowlands, D.D., Lemoine, F.G., Smith, D.E., and Zuber, M.T., 2001, Crossover analysis of Mars Orbiter Laser Altimeter data: Journal of Geophysical Research, v. 106, p. 23,753-23,768.

Platz, T., Michael, G.G., and Neukum, G., 2010, Confident thickness estimates for planetary surface deposits from concealed crater populations: Earth and Planetary Science Letters, v. 293, p. 388-395.

Robbins, S.J., and Hynek, B.M., 2012, A new global database of Mars impact craters ≥1 km: 1. Database creation, properties, and parameters: Journal of Geophysical Research, v. 117, doi:10.1029/2011JE003966.

Tanaka, K.L., Skinner, J.A., Jr., and Hare, T.M., 2009, Planetary Geologic Mapping Handbook (2009): in Abstracts of the Annual Meeting of Planetary Geologic Mappers, San Antonio, TX, 2009, NASA/CP-2010-216680.

Tanaka, K.L., Dohm, J.M., Fortezzo, C.M., Irwin, R.P., III, Kolb, E.J., Skinner, J.A., Jr., Hare, T.M., Platz, T., Michael, G., and Robbins, S., 2012, The geology of Mars: What the new global map shows: 43 Annual Lunar and Planetary Science Conference, The Woodlands, Texas, abstract 2702.

Figure DR1. Mapped unit mAl outcrops (gray) and associated landforms, as described in the text. The unit's maximum extent is represented by the dashed line and is based on the distribution and extent of pedestal-type craterforms (white dots) and thumbprint terrain (orange areas). Lettered arrow-boxes locate image panels in main text Figure 2. Numbered circles locate sites of modeled absolute ages (Table 1S). Narrow pink strips are CTX image footprints for areas examined in this study, from which a total of 4 counts yielded statistically sound model absolute ages. Transparent boxes distributed throughout the lowlands are full count areas summarized in Werner et al. (2011), from which a total of 7 counts yielded age values equivalent to those reported herein. MOLA color-shaded relief base in polar stereographic projection. 1:25,000,000 map scale.

Figure DR2. Detailed results from study-specific crater counts. Areas 1 through 4 are represented, each showing (1) crater size-frequency distributions, (2) model absolute basement and resurfacing ages, (3) CTX image used for counting, and (4) the population of craters identified in each area. Area 5, listed at the end of the figure sequence, provides an example of a statistically unsuitable count area, wherein crater size-frequency distributions transect model isochrons.

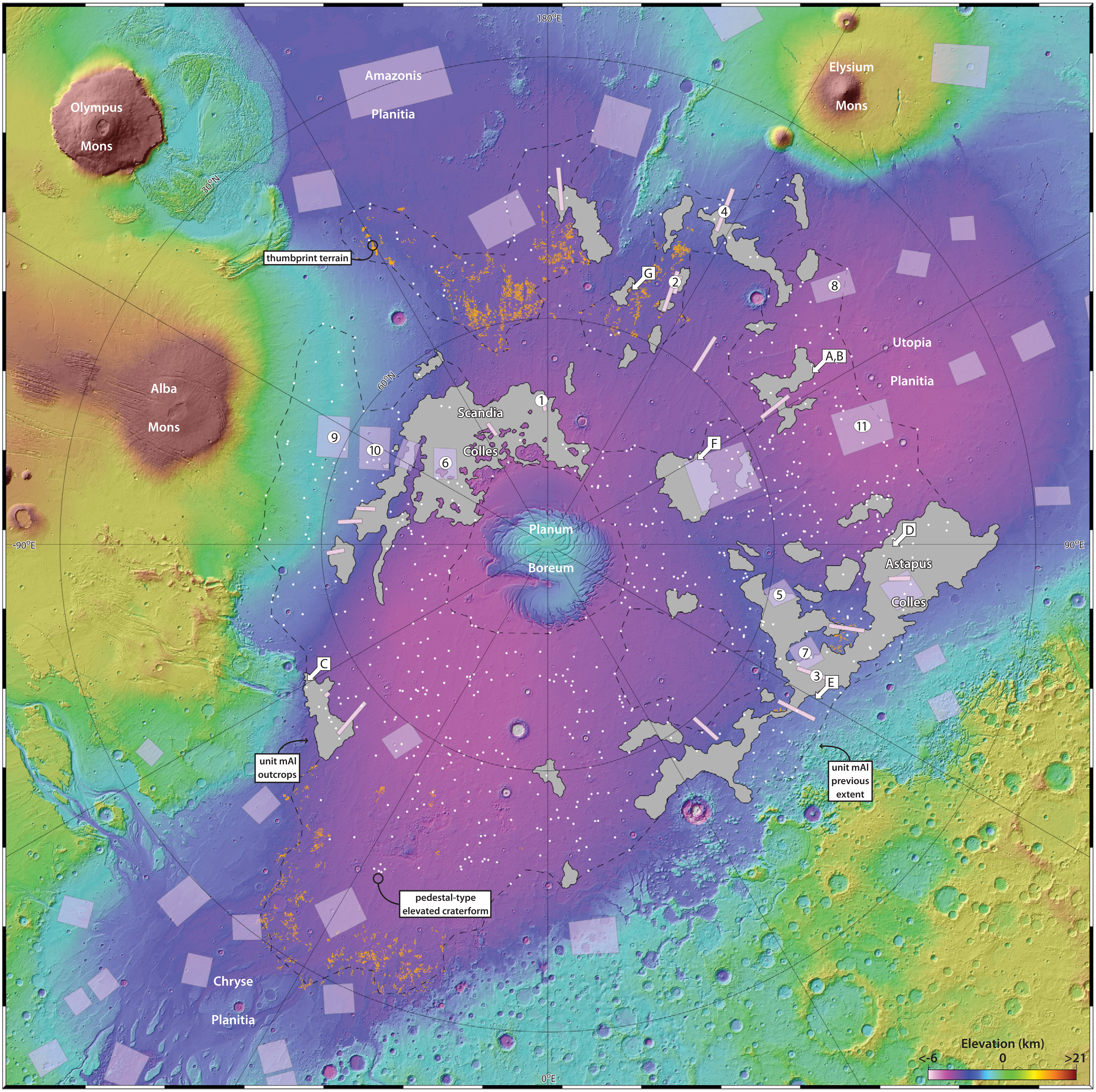

Map scale (at center) is 1:25,000,000

Polar Stereographic projection

MOLA shaded relief base

Supplement Figure DR1.

area 1

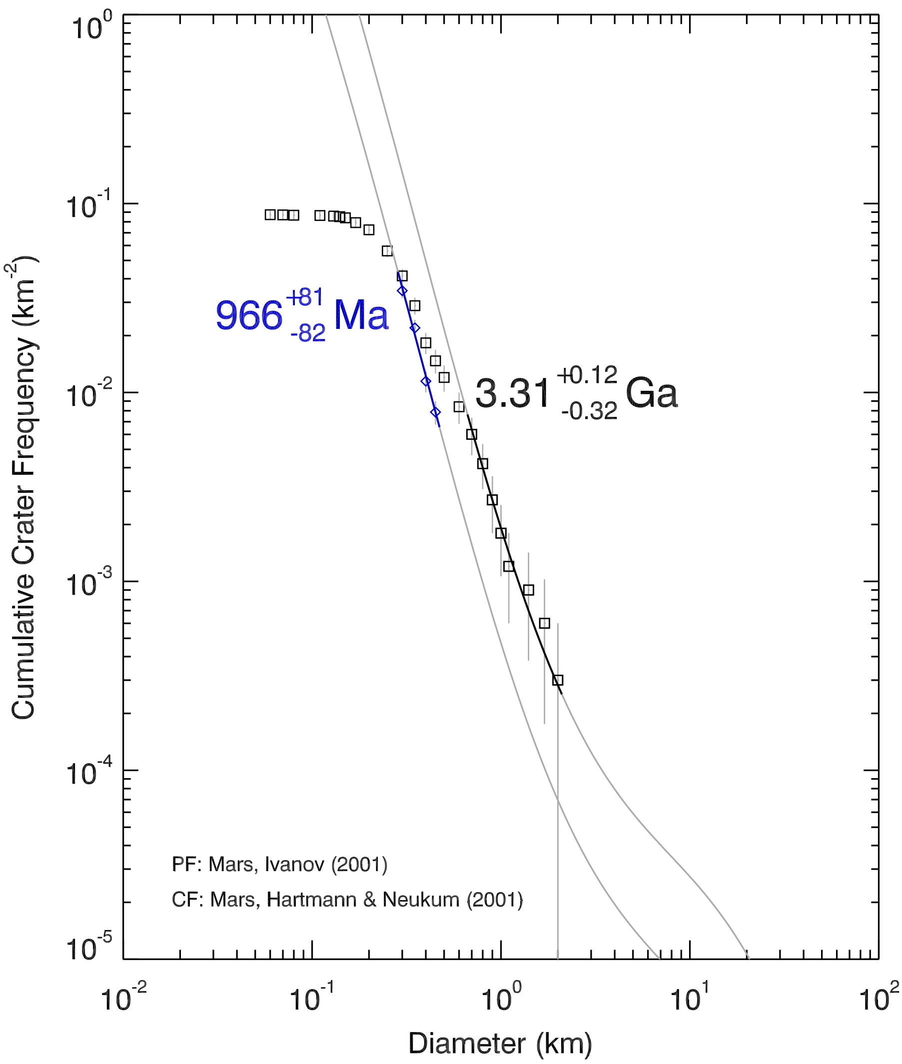

966 +81 -82 Ma
3.31 +0.12 -0.32 Ga
PF: Mars, Ivanov (2001)
CF: Mars, Hartmann & Neukum (2001)
Cumulative Crater Frequency (km^-2)
Diameter (km)

area 1

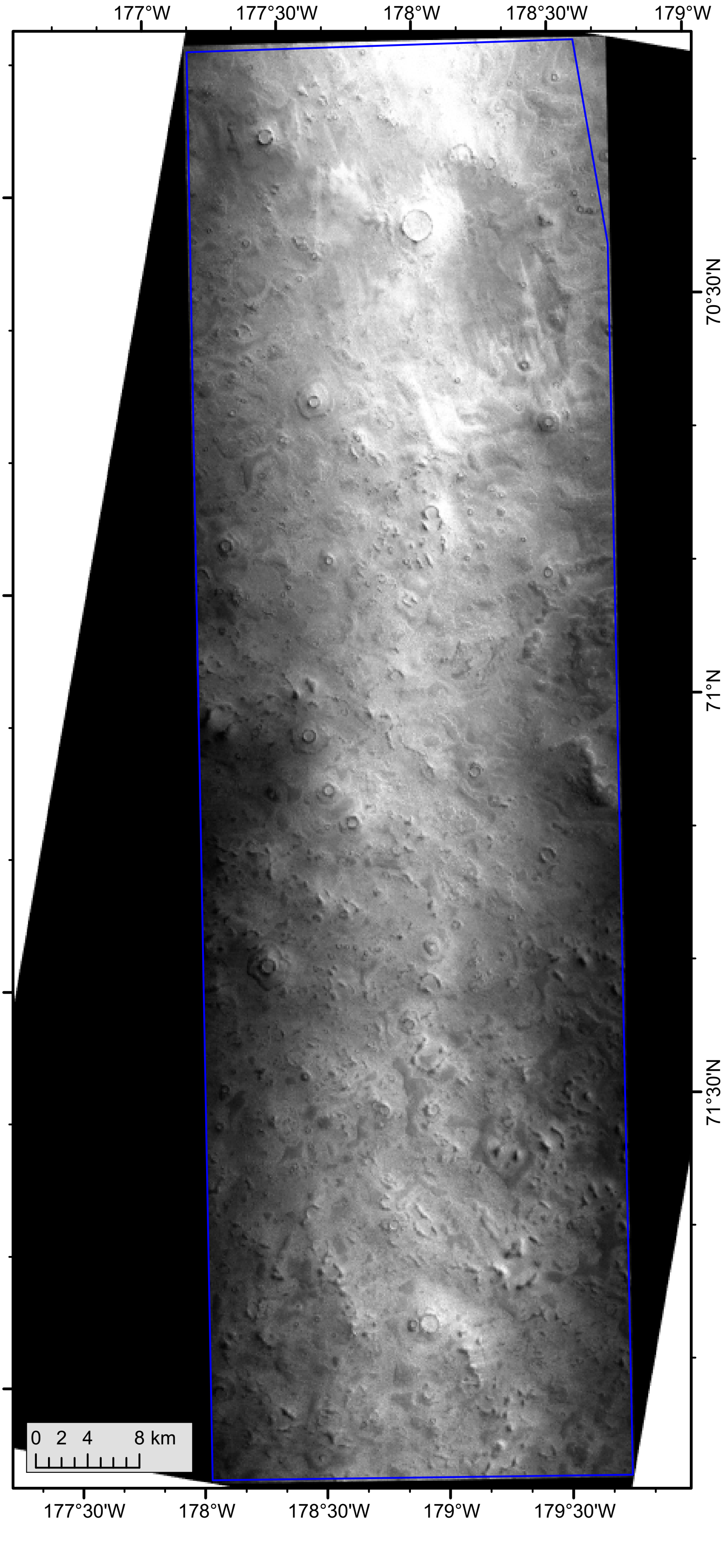

177°W
177°30'W
178°W
178°30'W
179°W
70°30'N
71°N
71°30'N
72°N
70°30'N
71°N
71°30'N
0 2 4 8 km
177°30'W
178°W
178°30'W
179°W
179°30'W

area 1

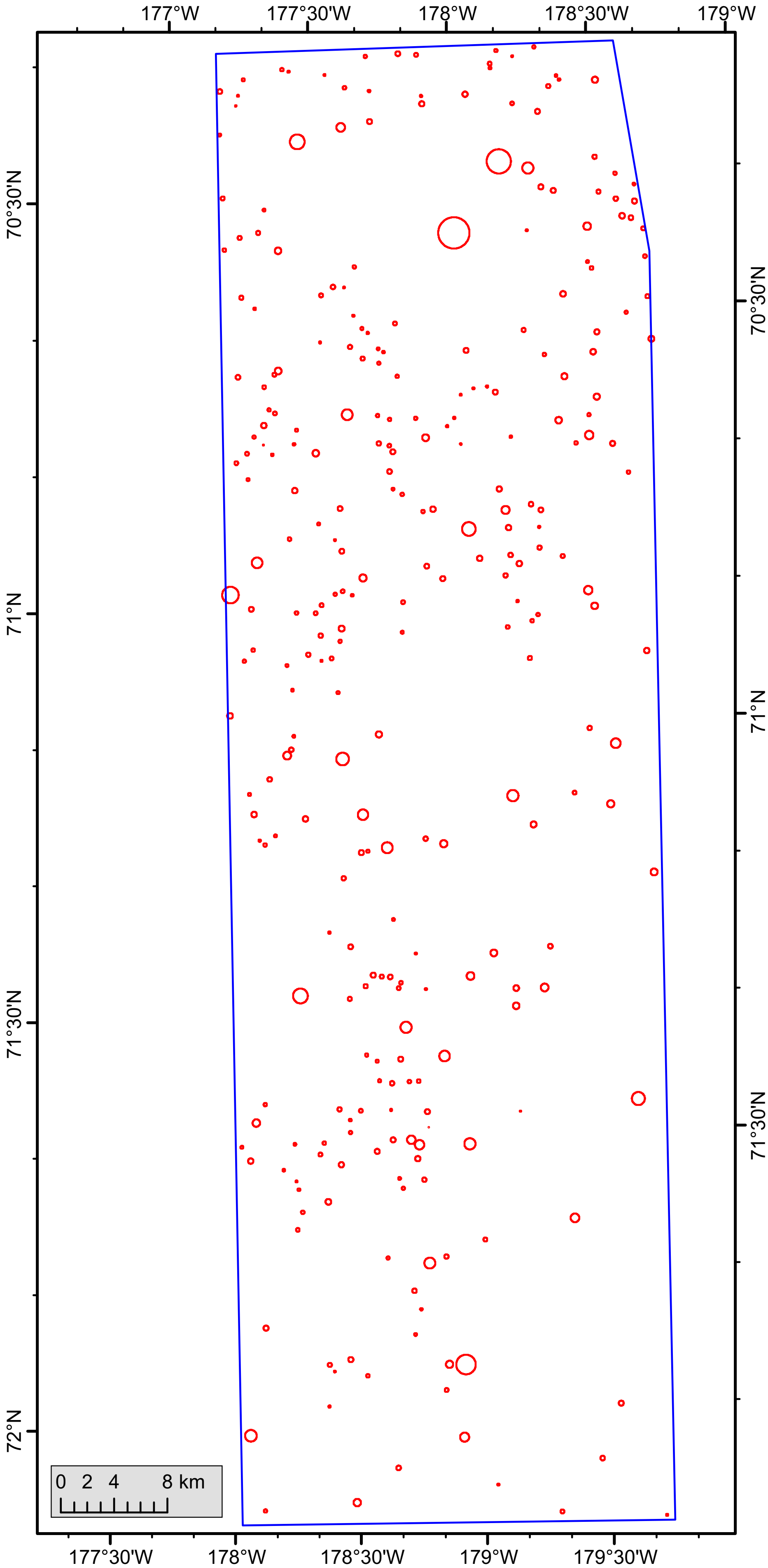

177°W
177°30'W
178°W
178°30'W
179°W
70°30'N
71°N
71°30'N
72°N
0 2 4 8 km
177°30'W
178°W
178°30'W
179°W
179°30'W
70°30'N
71°N
71°30'N

area 2

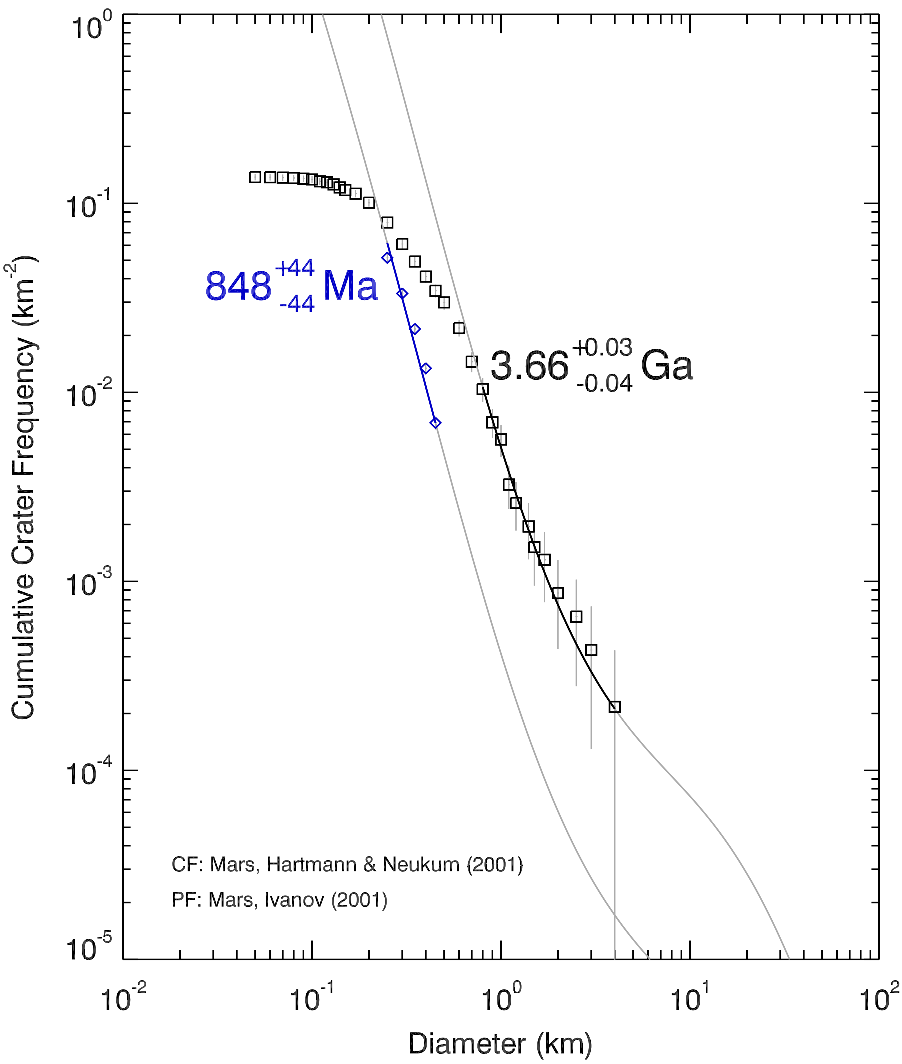

Cumulative Crater Frequency (km^-2)
Diameter (km)
848 +44 -44 Ma
3.66 +0.03 -0.04 Ga
CF: Mars, Hartmann & Neukum (2001)
PF: Mars, Ivanov (2001)
10^0
10^-1
10^-2
10^-3
10^-4
10^-5
10^-2
10^-1
10^0
10^1
10^2

area 2

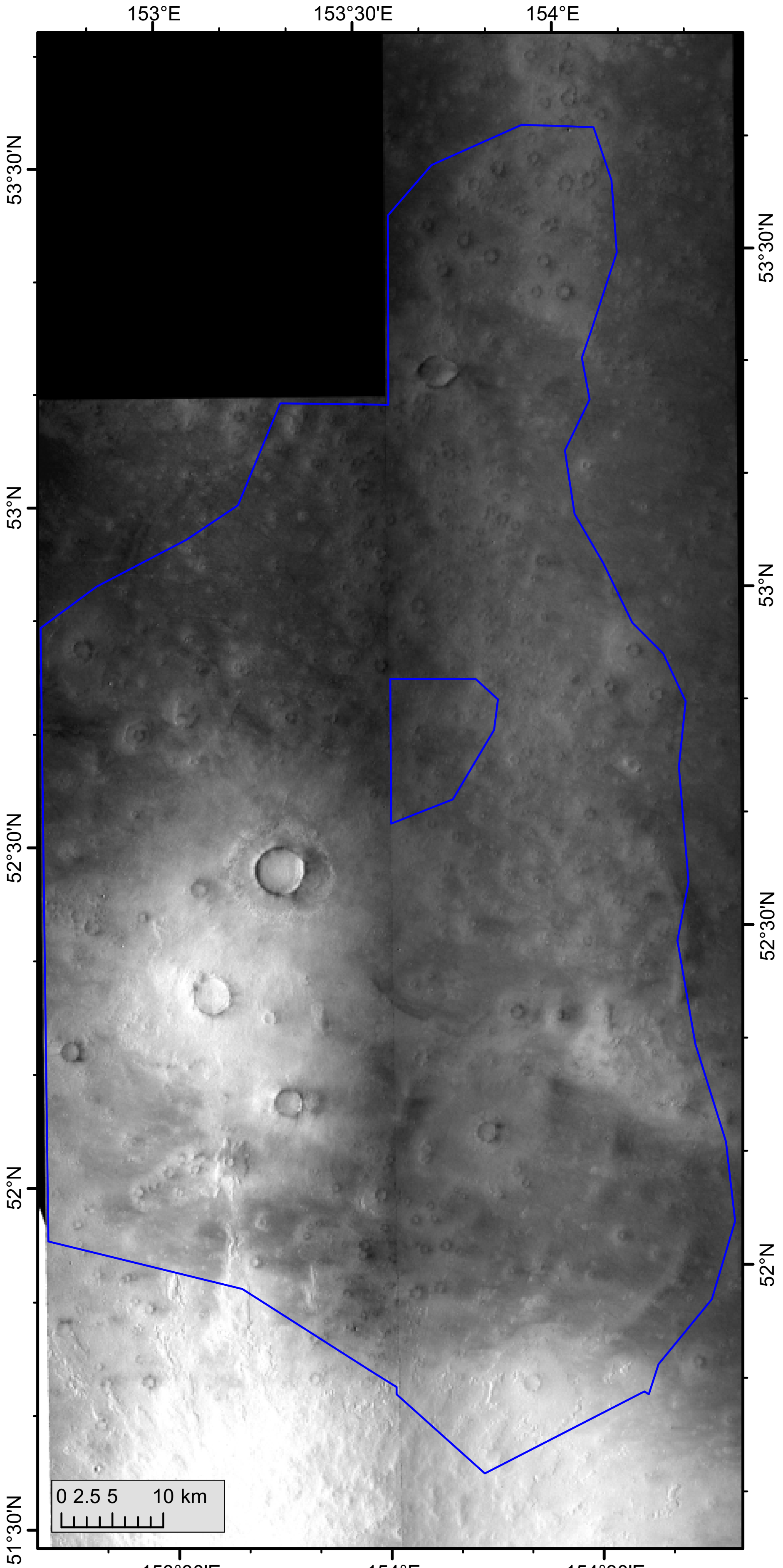

153°E
153°30'E
154°E
53°30'N
53°N
52°30'N
52°N
51°30'N
0 2.5 5 10 km
153°30'E
154°E
154°30'E

area 2

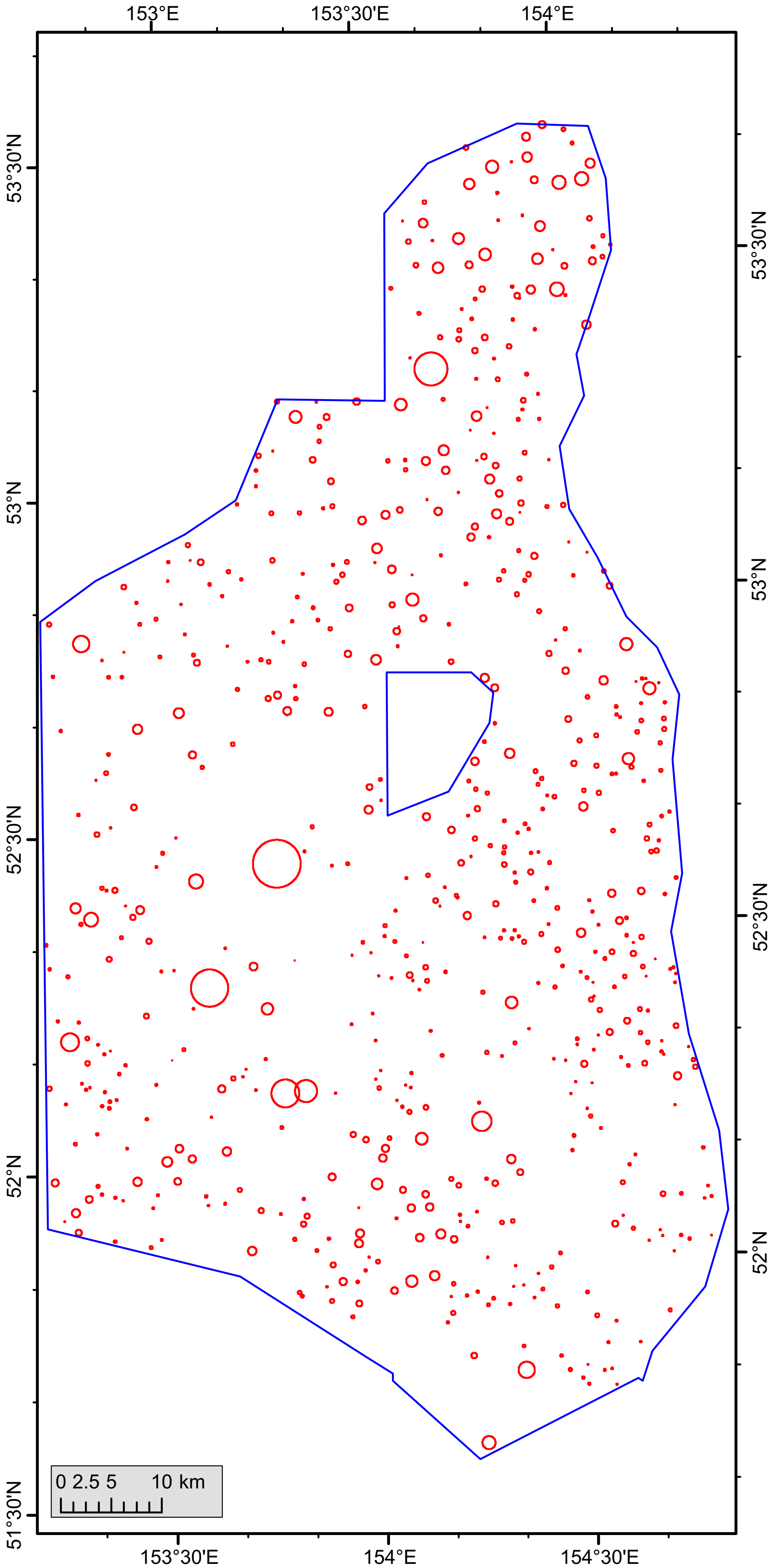
153°E
153°30'E
154°E
153°30'E
154°E
154°30'E
53°30'N
53°N
52°30'N
52°N
51°30'N
0 2.5 5 10 km

area 3

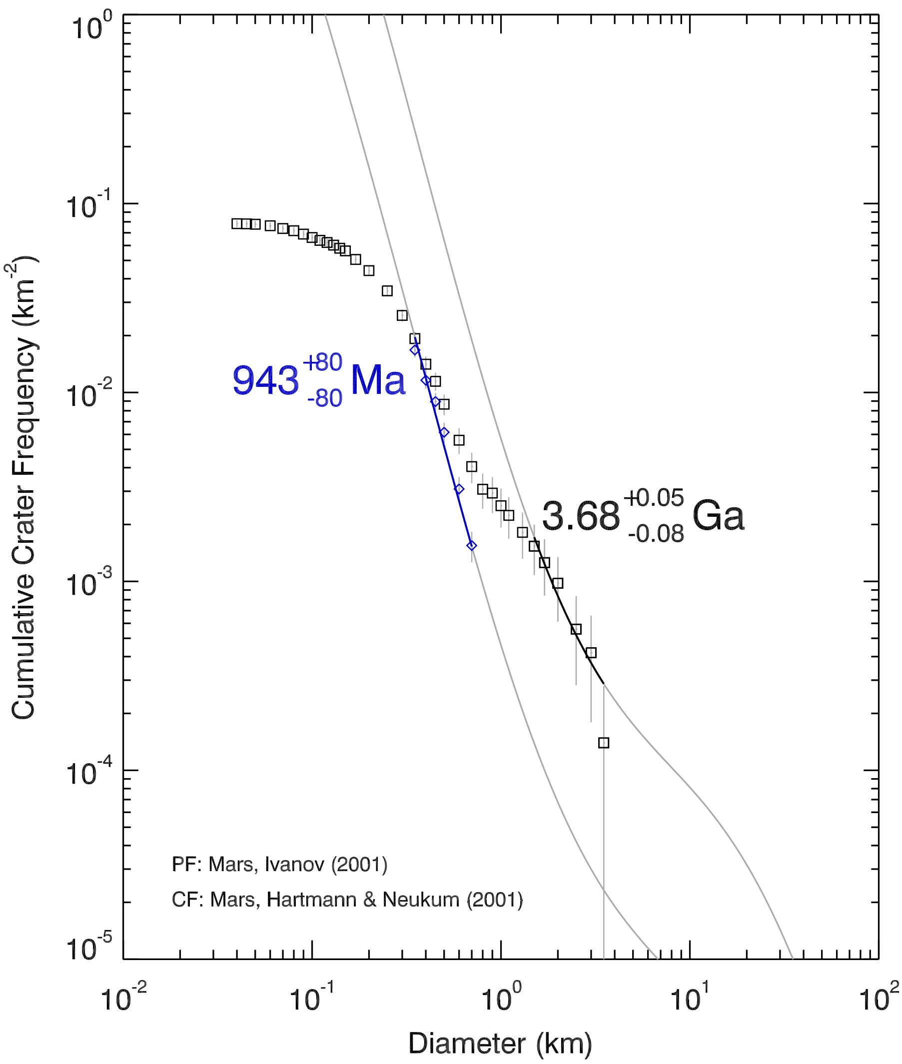

Cumulative Crater Frequency (km^{-2})
10^{0}
10^{-1}
10^{-2}
10^{-3}
10^{-4}
10^{-5}
943^{+80}_{-80} Ma
$3.68^{+0.05}_{-0.08}$ Ga
PF: Mars, Ivanov (2001)
CF: Mars, Hartmann & Neukum (2001)
10^{-2}
10^{-1}
10^{0}
10^{1}
10^{2}
Diameter (km)

area 3

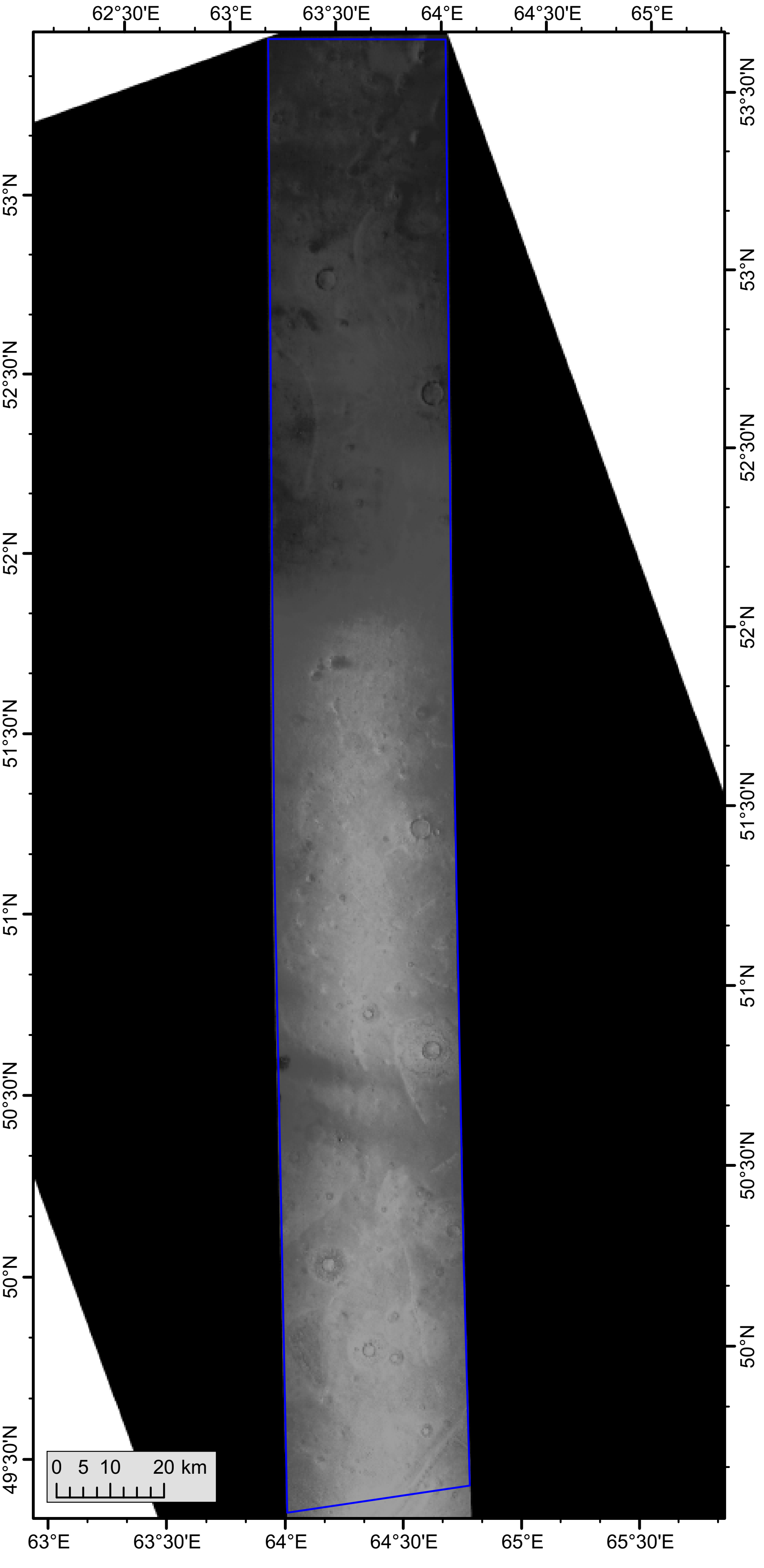

62°30'E
63°E
63°30'E
64°E
64°30'E
65°E
53°30'N
53°N
52°30'N
52°N
51°30'N
51°N
50°30'N
50°N
49°30'N
0 5 10 20 km
63°E
63°30'E
64°E
64°30'E
65°E
65°30'E

area 3

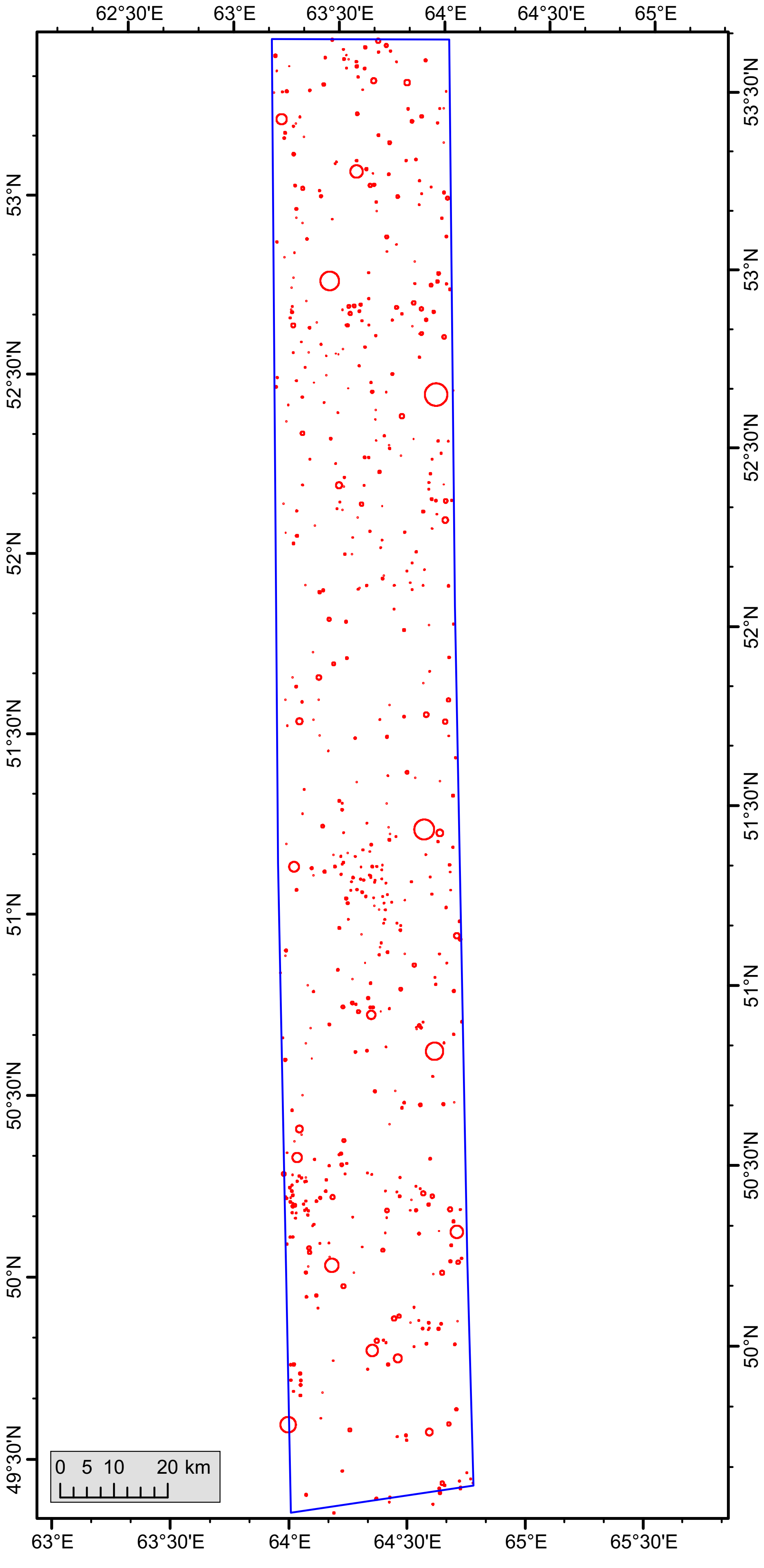

62°30'E
63°E
63°30'E
64°E
64°30'E
65°E
53°30'N
53°N
52°30'N
52°N
51°30'N
51°N
50°30'N
50°N
49°30'N
63°E
63°30'E
64°E
64°30'E
65°E
65°30'E
0 5 10 20 km

area 4

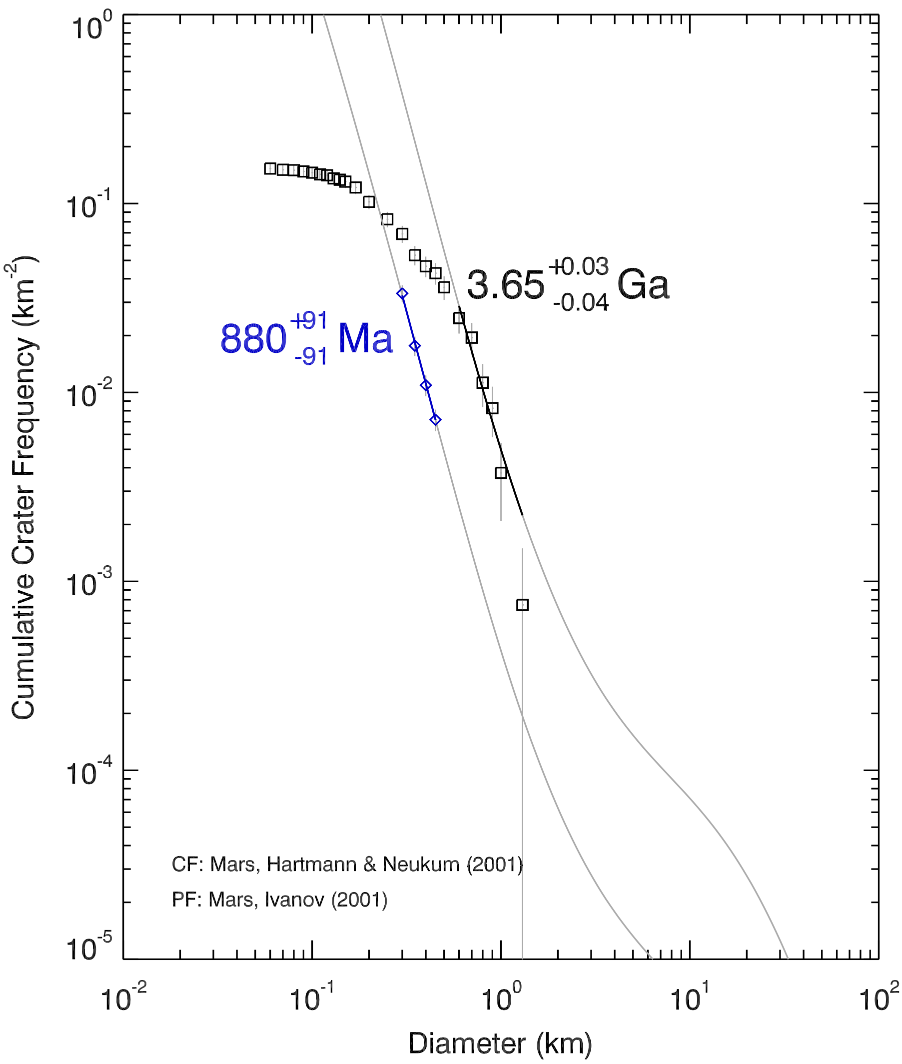

Cumulative Crater Frequency (km^-2)
Diameter (km)
3.65 +0.03 -0.04 Ga
880 +91 -91 Ma
CF: Mars, Hartmann & Neukum (2001)
PF: Mars, Ivanov (2001)

area 4

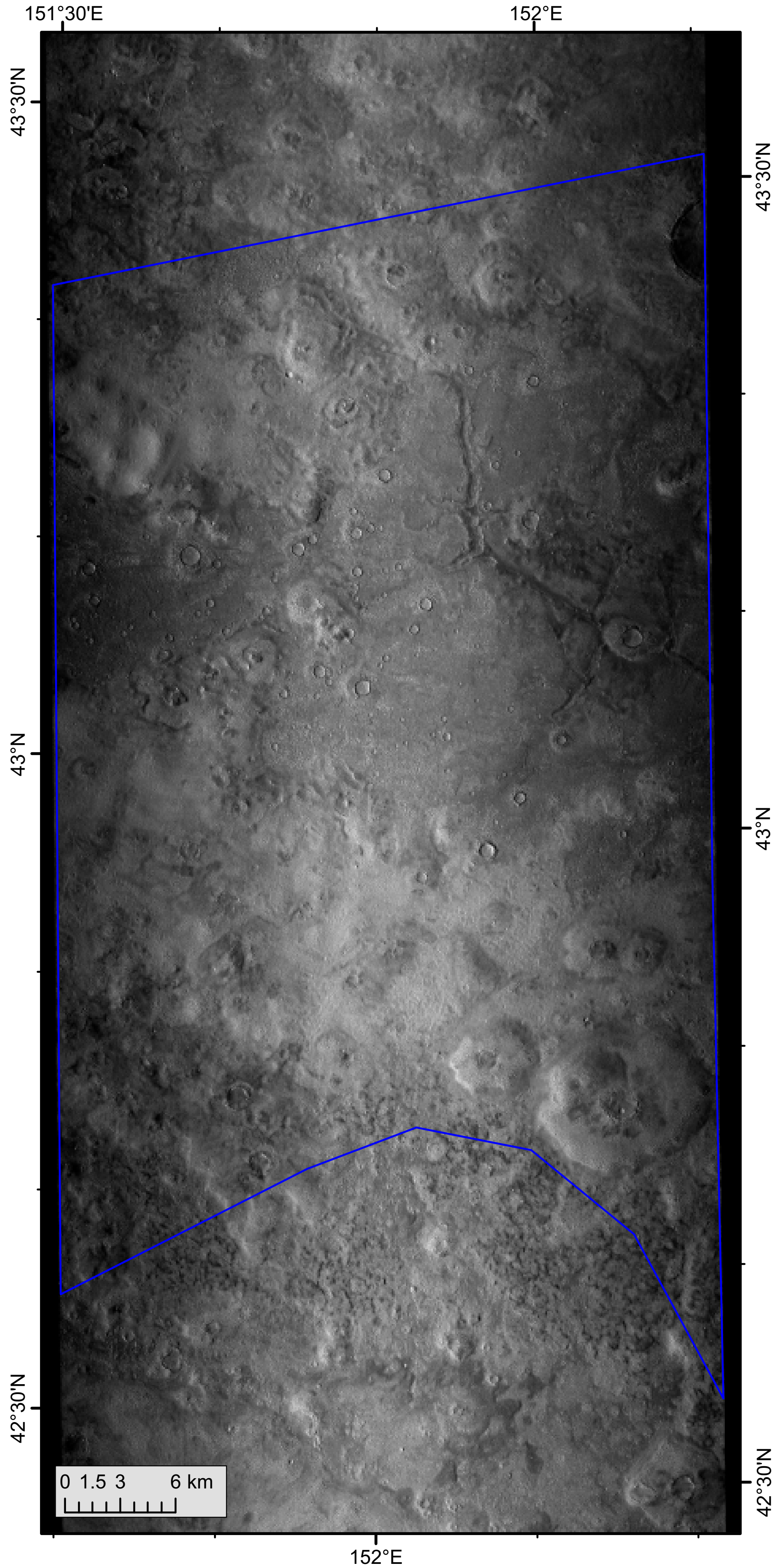

area 4

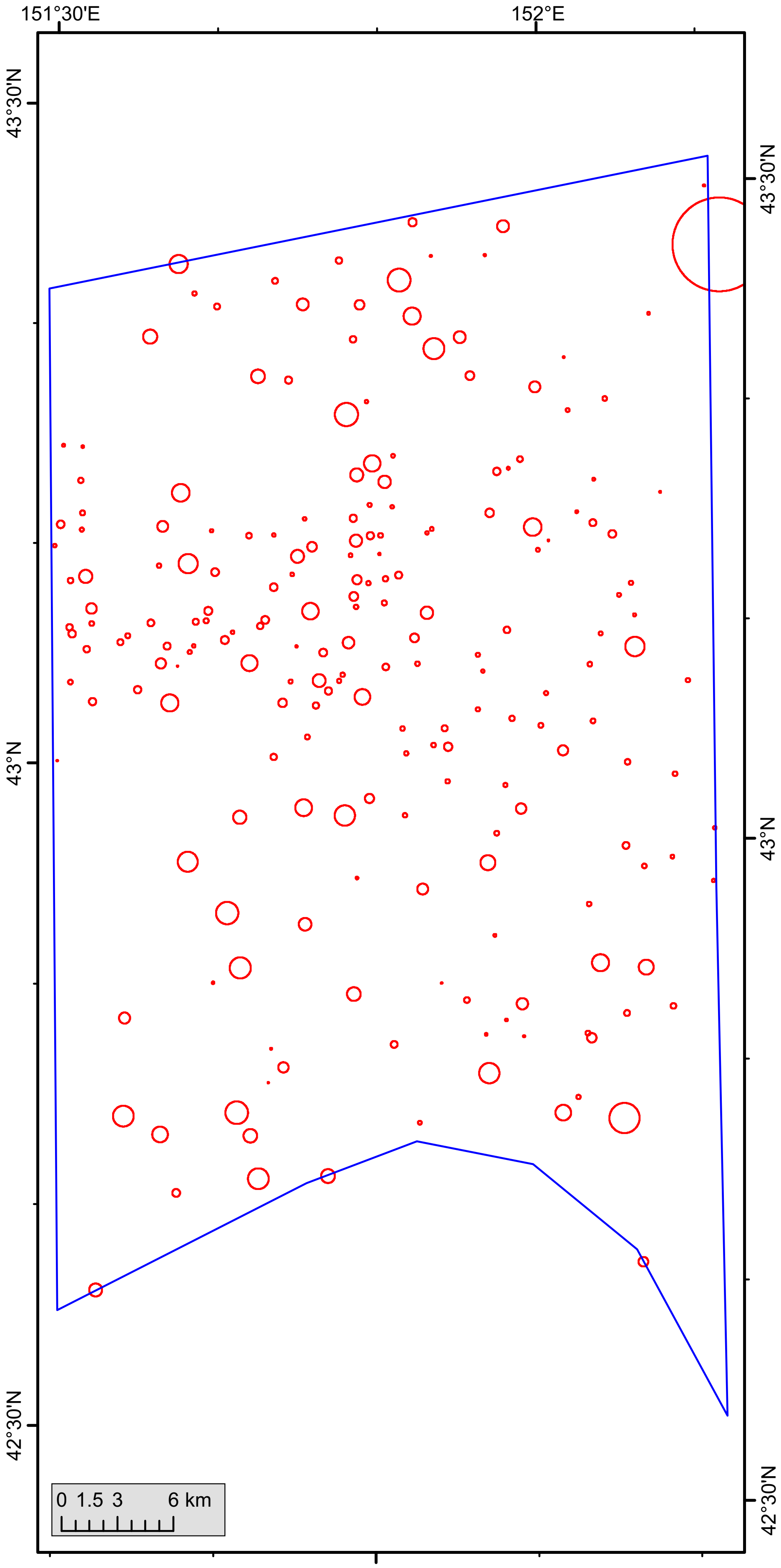

area 5 - unsuitable

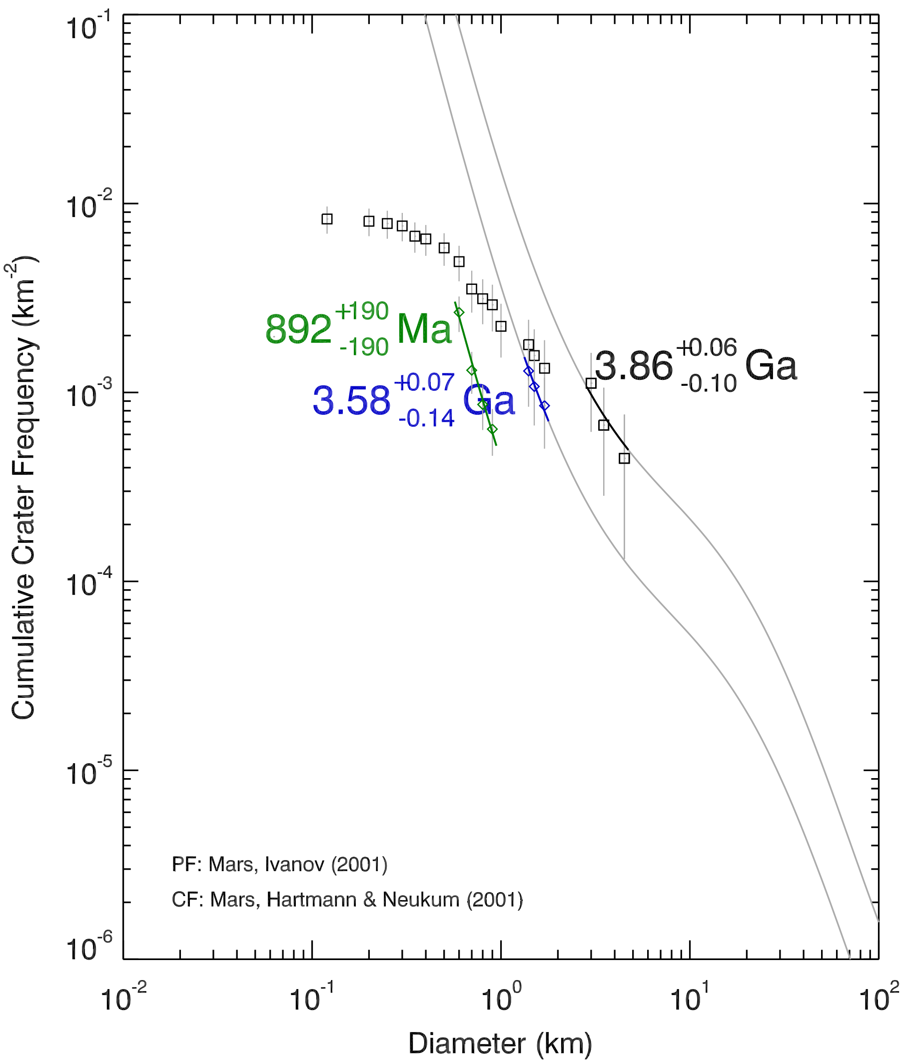

- only 37 craters were counted on an area of 4,470 km²
- many structures could potentially also be impact craters
- in many cases crater diameters are not determinable

area 5 - unsuitable

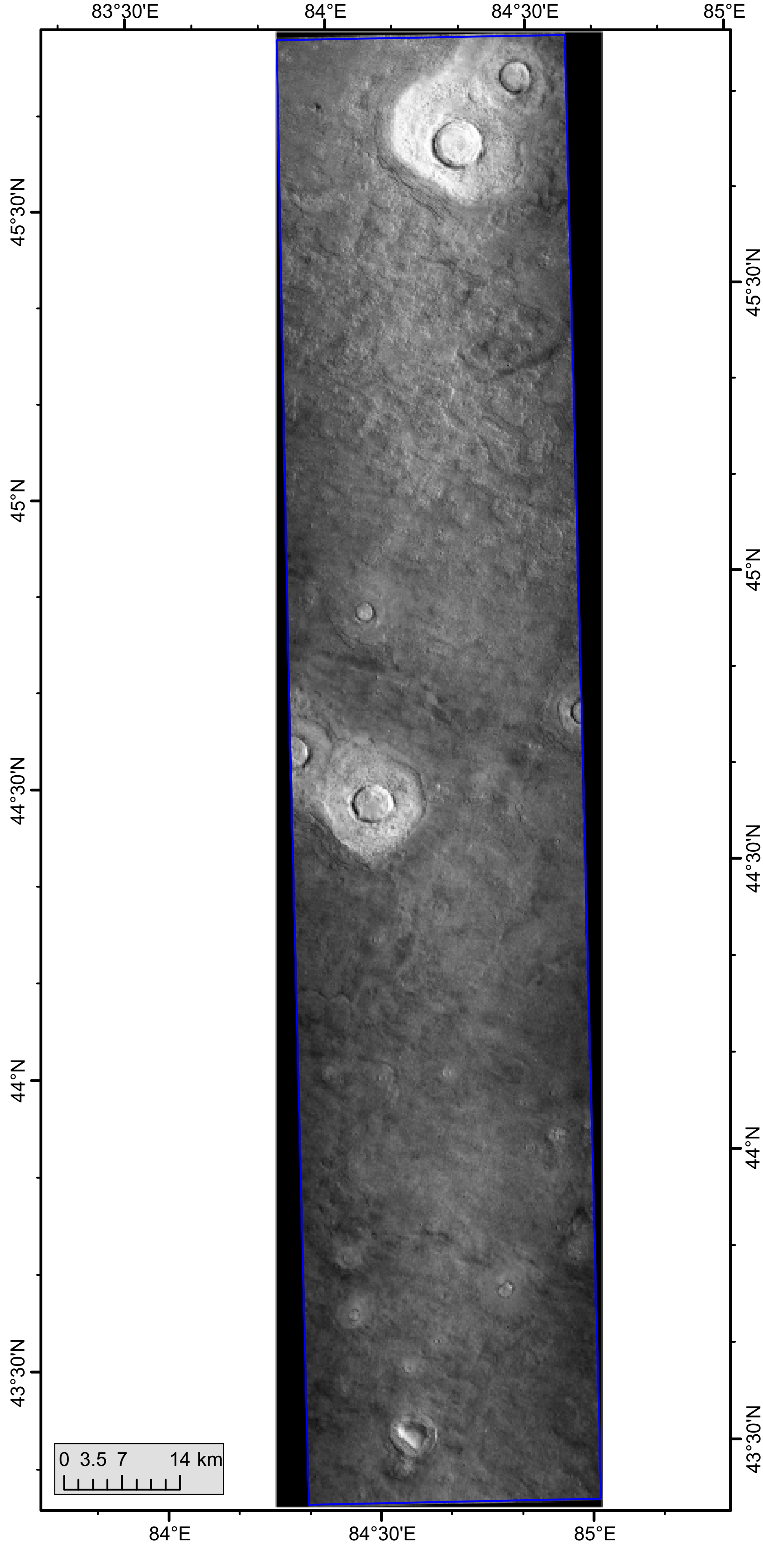

area 5 - unsuitable

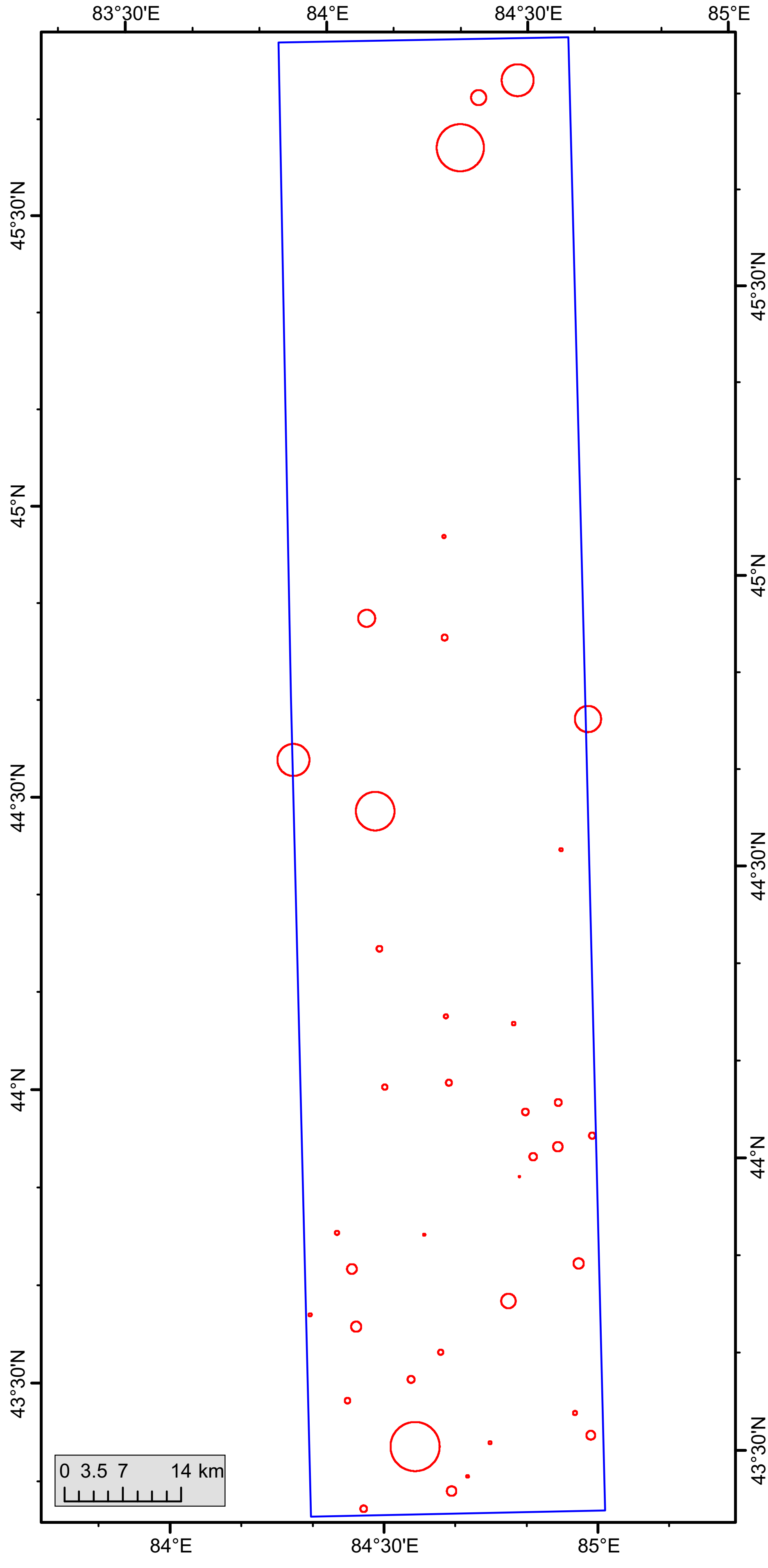

area 5 - unsuitable

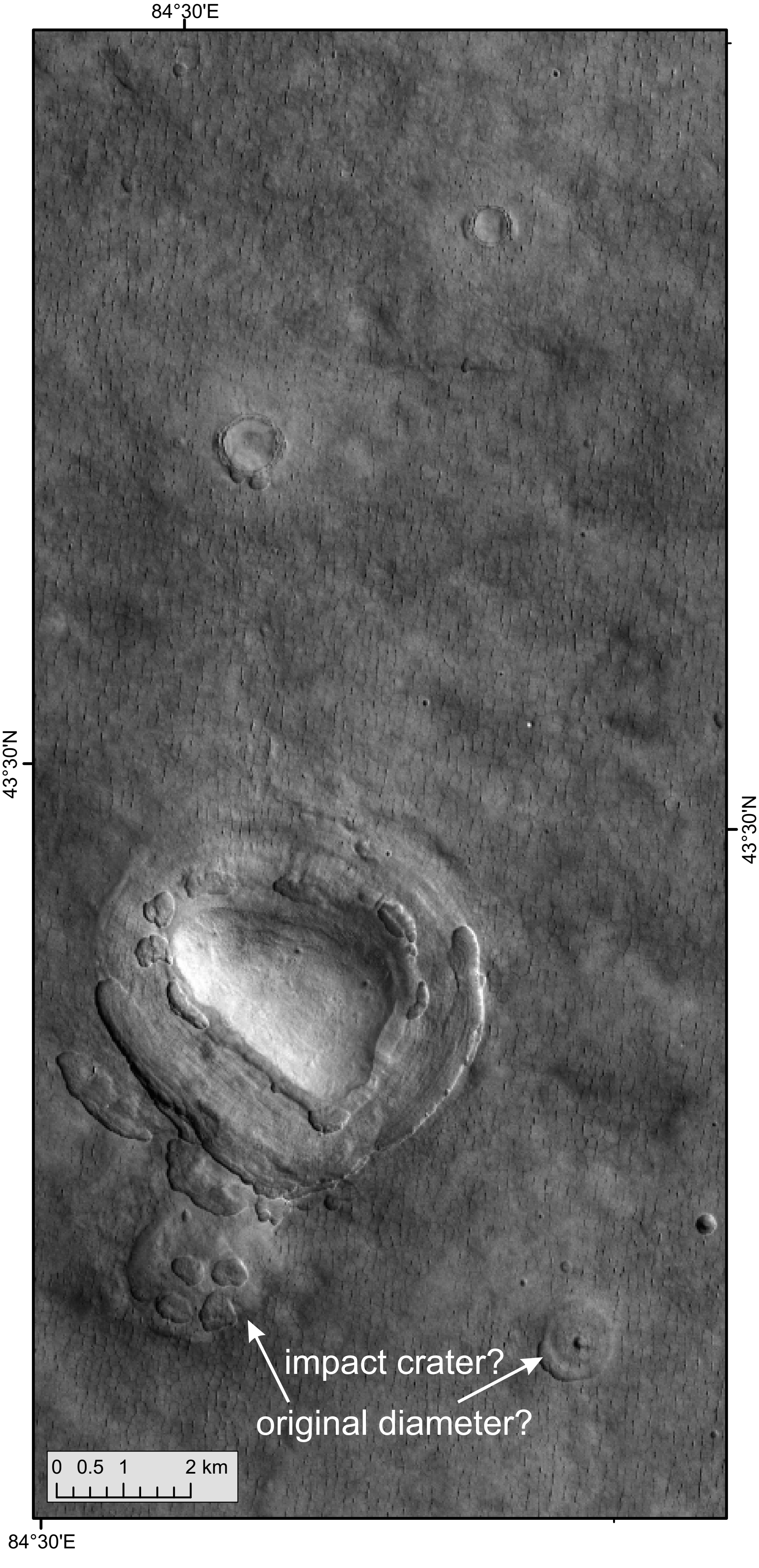

area 5 - unsuitable